Indentation tectonics in nature and experiment.
1. Experiments scaled for gravity

P. DAVY AND P.R. COBBOLD

Patterns of faulting and lithospheric thickening resulting from indentation of one continent by another have been investigated using experiments scaled for gravity. The experimental models have 2 or 3 lithospheric layers resting upon an asthenosphere. Densities are chosen to represent crust and mantle. The upper crust is brittle, with Navier-Coulomb frictional behaviour; other layers are viscous. Viscosities are attributed on the basis of currently estimated strength profiles for a 3-layer lithosphere. Model continents are indented by rigid or deformable indenters under various conditions of lateral constraint and in a normal gravity field.

Indentation results in different patterns of faulting and crustal thickening, depending mainly upon the degree of lateral confinement, but also upon layer rheologies and the dimensions of indented and indenting continents. Strong lateral confinement leads to crustal thickening alone, localized in a plateau region in front of the indenter. The main mechanism of thickening and of plateau accretion is a serial northwards propagation of thrusts in the uppermost brittle layer. Individual thrusts are arcuate and slip vectors are radial, leading to arc-parallel extension in the hangingwalls of forethrusts and arc-parallel contraction in the hangingwalls of backthrusts, with associated block rotations about vertical axes.

Weak lateral confinement at an eastern margin favours eastwards lateral escape, but some thickening also occurs near the indenter. Faults are dominantly wrenches and rifts. A main left-lateral wrench zone, between the indenter and the unconfined margin, separates the area of eastwards escape from undeformed continental material.

Moderate lateral confinement at an eastern margin results in both thickening and lateral escape, in roughly equal proportions. Thickening is concentrated in a plateau area in front of the indenter. Lateral escape is facilitated by a main left-lateral wrench zone, joining the western corner of the plateau to the eastern continental margin. This wrench zone is convergent in the SW and divergent in the NE. It contains synthetic wrench faults and can also contain antithetic ones that rotate by a domino mechanism.

In spite of large indenter displacements, none of our experiments showed serial eastwards escape of successive continental blocks, as occurs in experiments where plane-strain is artifically imposed.

P. Davy and P.R. Cobbold, Centre Ammoricain d'Etude Structurale des Socles (CNRS), Université de Rennes 1, 35042 Rennes Cedex, France, received 15th August 1987; revision received 3rd March 1988.

Introduction

It is now clear that continental collision can result, not only in mountain ranges at continental margins, but also in large areas of more diffuse deformation well within continents. This is especially visible in Central Asia. The very earliest geological data led Argand (1924) to several inescapable conclusions: Cenozoic deformation, mainly faulting, has occurred throughout an area of some 10^6 Km^2; it has resulted from the indentation of Asia by India; and it accounts for most of the current mountain ranges and high plateaux of Central Asia. Molnar & Tapponnier (1975) used seismic data and satellite im-

agery to show that indentation is active today. After continental collision some 50 Ma ago, the Indian plate has advanced some 2 500 Km northwards into Asia, at an average rate of about 5 cm.a^{-1}. Thus an interesting problem is why deformation has been so widespread in Central Asia.

Another problem in Central Asia is to know how indentation has been accommodated. Has it been accommodated by (i) crustal thickening, as advocated for example by Argand (1924), England (1982) or England & Houseman (1986); (ii) or by lateral escape (horizontal expulsion) of parts of China or S.E.Asia (Tapponnier et al., 1982)? For Asia, the best answer will be provided one day by
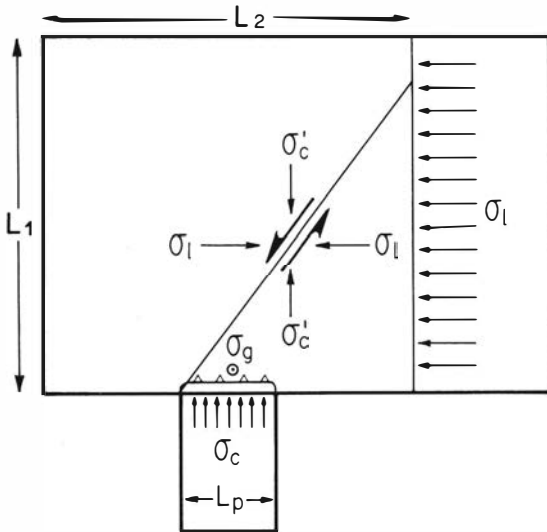
Fig. 1. Schematic model of continental indentation. Indenter (lower rectangle) advances northwards (up) into continent, causing thrusts (triangles on hangingwall) and strike-slip faults (double arrows). Width of indenter is L_p, effective width of continent is L_2. Thrust is generated in front of indenter when horizontal principal compressive stress (σ_c) overcomes vertical gravitationally-induced minimum compressive stress (σ_g) plus resistance of material. Within continent, (σ_c) becomes more diffuse; we assume $\sigma_c' = \sigma_c\ (L_p/L_2)$. Strike-slip fault is generated when σ_c' overcomes lateral confining stress (σ_l) plus resistance of material. This leads to lateral escape. All quantities are assumed vertically averaged over the entire lithosphere.

the wealth of geological and geophysical data that is accumulating. An integrated approach to this problem and some tentative answers based on currently available data are presented in the second paper of this series. In particular, we look at the surface fault pattern, because crustal thickening must involve thrusting, whereas lateral escape must involve wrenching or rifting.

Another approach, which is particularly valuable at the moment on account of its predictive capacity, is to model the process of indentation, mathematically, numerically and experimentally. A certain number of models have already been described or applied and the purpose of this paper is to provide additional ones, and to investigate the influence of lithospheric rheology and boundary conditions upon the mechanisms of indentation (Fig. 1). We believe the results will be of interest, not only for Asia, but for continental indentation in general.

Previous models

The earliest mathematical models to be applied to Central Asia were plane-strain solutions for instantaneous slip-line fields derived from the theory of plasticity (Tapponnier & Molnar, 1976). In such solutions, indentation produces two families of curved slip-lines, which show some similarity with strike-slip faults identified by Molnar & Tapponnier (1975) on satellite photographs of Asia. This theory cannot account for thrusts of rifts because of the assumption of plane strain. We will show later how this assumption can be relaxed to account for the intiation of arcuate thrusts.

Because the simple instantaneous slip-line fields are inappropriate for modelling a progressive deformation leading to finite slip upon structural weaknesses, Tapponnier et al (1982, 1986), Peltzer (1987) and Peltzer & Tapponnier (in press) did a series of indentation experiments, using plasticine, under conditions, once again, of plane strain. The experiments showed how individual faults, once formed, have long histories as structural weaknesses, contributing in a special way to the bulk kinematics. The extreme conditions of plane strain, while avoiding the need to scale the experiments for gravity, result inevitably in indentation being taken up entirely by lateral escape. However, these experiments did show how such escape is primarily eastwardly directed if the eastern margin of the model is unconstrained.

Similar results at regional scale were obtained by Vilotte et al (1982) using two-dimensional numerical calculations with non-linear viscous behaviour under the assumption of plane strain. Although here of course the role of individual faults cannot be appreciated, these calculations confirmed the importance of constraint or lack of constraint at continental margins. Vilotte et al (1982) also investigated conditions of plane stress and obtained very different results: crustal thickening now played a dominant role in the deformation pattern.

The first serious attempt at incorporating gravitational forces in viscous numerical calculations was made by England & McKenzie (1982, 1983) and England (1982) at the expense of some simplifications; notably a neglect of shear stresses acting upon horizontal planes. Refinements to the method were provided by Houseman & England (1986); but their calculations, although incorporating a non-linear dependance of strain-rate upon stress, included no strain-softening or other features leading to faults or narrow zones of permanent weakness. Furthermore, Houseman & England (1986) did not investigate conditions of unconstrained margins and hence, not surprisingly, their calculations show pla-

teau areas of crustal thickening in front of the indenter. In contrast, Cohen & Morgan (1987) investigated unconstrained margins and observed diffuse lateral escape.

To extend the scope of available models, we decided to use physical models, scaled for gravity, built with a minimum of two lithospheric layers and one asthenospheric layer. We were able to use both brittle and ductile layers and investigate various conditions of constraint at lateral margins. So far we have performed 13 experiments and here we present the results of 9 of them. Further work (in progress) shows that these preliminary results are reproducible and that quantitative conclusions can be drawn.

By a suitable choice of model materials, we were able to conduct our experiments in a normal gravity field, without the use of a centrifuge. We draw the reader's attention to the recent experimental work of Peltzer (1987, and this volume) which did make use of a centrifuge.

Experimental method

Properties of lithosphere

The rheology of the continental lithospheric is currently a subject of debate. Estimates have been made using data obtained from experimental deformation of rocks under laboratory conditions (see, for example, Heard 1976, Carter 1976, Kirby 1983 for raw data and Goetze and Evans 1979, Brace and Kohlstedt 1980, Molnar and Tapponnier 1981, Kirby 1985, Ranalli and Murphy 1987, Tsenn and Carter 1987, Carter and Tsenn 1987 for application to lithospheric strength).

On this basis, it seems likely that the uppermost crust (and possibly the uppermost mantle at low thermal gradients) behaves in a brittle fashion, according to the laws of friction, so that brittle strength increases with depth. In contrast, the lower crust and much of the mantle may behave in a more viscous fashion, strength depending nonlinearly upon strain rate and upon temperature.

For the present series of experiments, we assume that the continental lithosphere is adequately represented by at most four layers: brittle upper crust, ductile lower crust, high-viscosity mantle and low-viscosity mantle (asthenosphere). We have used this fourfold subdivision to calculate, on the basis of experimental data, the mean resistance of each lithospheric layer. The method and its application to mechanisms of crustal thickening are discussed by Davy (1986) and Davy & Cobbold (work in progress).

Scaling

At lithospheric scale, gravitational forces cannot be neglected. Hence in a physical model designed to reproduce lithospheric deformation, gravitational forces should be correctly scaled in relation to surface forces (Hubbert 1937, Ramberg 1967). In practical terms, this means that, if we want to use a normal gravitational field, quantities with the dimensions of stress must be scaled down by the same factor as the linear dimensions. For brittle material obeying a Navier-Coulomb law, the cohesion has the dimensions of stress and must therefore be scaled down in the model; whereas the coefficient of internal friction, being dimensionless, must be the same in model and in nature. In practice, in a model where 1 mm represents 10 000 Km (a length ratio of 10^{-7}), cohesion must be negligibly small, whereas internal friction should have a coefficient of about 0.6, as in real rocks under lithospheric conditions (see Horsfield 1977 and Vendeville et al. 1987 for further discussion). Hence rock is adequately modelled by a dry granular material, such as ordinary quartz sand.

For ductile layers, strength depends upon strain-rate and so we need to consider the time scale. This is best chosen on a practical basis, so that an experiment does not last more than a few days. We use a time ratio of about 10^{-10} (1 hour represents 1 Ma). This means that quantities with the dimensions of viscosity are scaled down by a factor of about $10^{-10} \times 10^{-10} = 10^{-17}$. Under these conditions, a lower crustal layer with a viscosity of 10^{21} Pa.s is adequately represented by a model material with the consistency of pitch (10^4 Pa.s); also a plate velocity of 5 cm.a^{-1} scales up in the model, by a factor of about $10^{-7}/10^{-10} = 10^3$, to a value of about 1 cm. hr^{-1}.

Model materials

Brittle upper crust was modelled using quartz sand. We used a naturally occurring uncemented sand of aeolian origin from Fontainebleau (France). Quartz grains are well rounded. We sieved the sand and retained the fraction below 0.2 mm. After washing and drying, various batches were coloured using organic or mineral pigments. The density of this sand is about 1.3 g cm^{-3}, depending upon the degree of compaction. It was reduced to about 1.2 g cm^{-3} by admixture with powdered ethyl cellulose. The mixture fails according to a Navier-Coulomb frictional law, with a coefficient of about 0.6 and a negligible cohesion. Shear failure occurs along faults (in fact, narrow shear zones) where progressive dilation

Table 1. Materials in nature and experiment. Sand is a purely brittle material obeying a Navier-Coulomb law with angle of internal friction (ϕ = 30°) and negligible cohesion (C = O). Silicones and glucose syrup are newtonian viscous fluids (μ = viscosity). Chosen densities (d) ensure a gravitationally stable initial layering and are in correct proportion for crust and mantle.

Layer	Lithospheric Materials	Modelling Materials	Physical properties	Model
1	Brittle Crust	Sand	Navie-Coulomb ϕ=30°,C=0 Pa d=1.2 g.cm⁻³	1,2,3,4,5 6,7,8,9
2	Ductile Crust	Silicone 1	Newtonian μ=1.5 10⁴ Pa.s d=1.2 g.cm⁻³	1,2,3,4,5 6,7,8,9
3	High-viscosity Mantle	Silicone 2	Newtonian μ=2 10⁵ Pa.s d=1.4 g.cm⁻³	6
4	Low-viscosity Mantle	Glucose Syrup	Newtonian μ=10 Pa.s d=1.4 g.cm⁻³	1,2,3,4,5 6,7,8,9

Table 2. Initial dimensions and measures of resistance of models (ho = crustal thickeness, L_1 = length of continent, L_2 = width of continent, L_p = width of indenter, r = calculated ratio of brittle to ductile resisting forces, R = calculated ratio of maximum and minimum horizontal compressive stresses.

Model	ho (cm)	L_1 (cm)	L_2 (cm)	L_p (cm)	r=f_b/f_d	R=σ_c'/σ_1
1	1.0	100	60	20	20	∞
2	1.3	50	40	20	20	∞
3	1.3	50	40	20	20	240
4	1.3	50	40	10	20	120
5	1.3	70	40	10	20	120
6	1.3	70	40	10	1	7.5
7	1.3	50	40	20	20	<3
8	1.3	50	40	20	20	<3
9	1.3	50	40	20	20	<3

causes strain-softening and hence localization, as in pure quartz sand (Mandl et al. 1977).

Viscous lithospheric layers were modelled using two silicone putties of different viscosities and densities. The basic material (silicone 1 in Table 1) is Gomme 7007, manufactured by Rhone-Poulenc, France. At room temperature this has a density of about 1.2 g.cm⁻³ and a viscosity of about 3×10^4 Pa.s. It is almost perfectly newtonian at the experimental strain-rates (less than 10^{-4} s⁻¹). It was used to model the lower crust (Table 1). High viscosity mantle was modelled using another silicone putty (silicone 2, Table 1) of higher density (about 1.4 g.cm⁻³) and higher viscosity (about 2×10^5 Pa.s), obtained by mixing the basic material (silicone 1) with finely powdered galena. This material was used in Model 6 only (see Table 1).

Finally mantle asthenosphere was modelled using glucose syrup. Again, this is newtonian, with a viscosity of about 10 Pa.s and a density of about 1.4 g.cm⁻³.

Model construction

Models were built layer by layer, from bottom to top, using a stable density stratification. A transparent box (dimensions in Table 2) was used both to build each model and to indent it. The box was first filled to a depth of 10 cm with glucose syrup. Layers of silicone 1 and 2 were pressure molded to the required dimensions in a separate frame and then placed successively in position. Adherence between the layers was sufficient to expel any trapped air bubbles. Gravitational forces acting over a period of a day or so resulted in strictly horizontal layering throughout the model. Finally, an upper-

most sand layer was deposited by careful sedimentation of successive sublayers about 1 mm thick. This was achieved using a trough long enough to span the model in one direction. The trough was displaced in the other direction at a steady speed, and the rate of sand flow controlled via a slit of variable aperture.

In experiments with unconfined or partially confined continental margins, a thin plate was temporarily introduced during model construction to separate continental from oceanic domains. The plate was removed before the model was subjected to deformation.

Deformation

Models were deformed using rectangular indenters of various widths (L_p, Table 2). These were deep enough to indent the silicone and sand layers, without reaching through the glucose syrup to the bottom of the box. The indenters were driven at a steady speed of 1 cm hr⁻¹, using a screw jack powered by a computer-controlled stepper motor.

Observation of models

Faults and horizontal displacements of grids at the upper surfaces of models were monitored by time-lapse photography, using a 35 mm camera with a programmable back. Changes in crustal and lithospheric thickness were monitored using photographs with horizontal and oblique lines of view through the transparent side plates of the box and the asthe-

nosphere. Finally, at the end of each experiment, the sand layer was progressively stripped away, using a commercial vacuum cleaner fitted with a fine nozzle on the end of a flexible hose. This revealed the upper surface of the layer of Silicone 1, in other words the brittle/ductile transition. The operation proved invaluable in locating faults at depth and hence reconstructing their three-dimensional geometry.

Analysis of results

In this paper we present line-drawings (Figs. 3 to 7) made from photographs of the upper surfaces of the models (Fig. 2). The drawings show deformed grids (dotted lines) and fault traces (solid lines). Grid offsets and spacing were used, together with fault geometry at depth, to determine slip vectors and classify faults. From the deformed grids, various area parameters were calculated. The amount of indentation A_i is the continental area replaced by indenter material. The amount of lateral escape A_e is the area of continental material to the east of the line of longitude marking the original position of the eastern margin, less the area dragged northwards with the indenter from the line of latitude marking the original position of the southern margin. The amount of continental thickening, A_t is the amount of indentation A_i less the amount of lateral escape A_e. Finally the ratio $S = A_e/A_t$ expresses the relative amounts of escape and thickening.
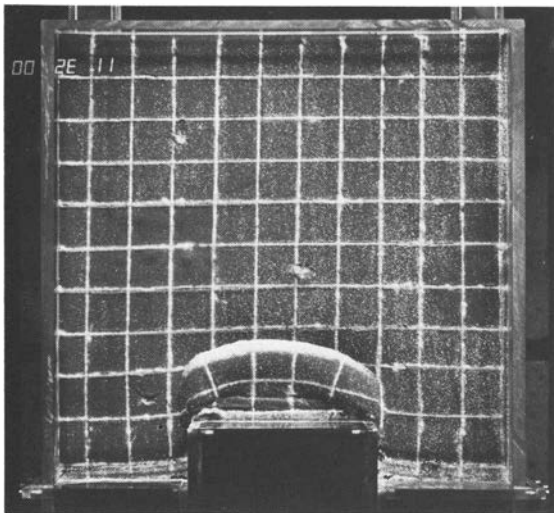

Fig. 2. Photograph of upper surface of Model 7 after indentation, showing square grid of marker lines and arcuate traces of thrust faults in front of rectangular indenter. For line drawing of same, see Fig. 3, top row.

Experimental results

1. Short continent, wide piston, various lateral confinements

In a first series of three experiments, only the strength of lateral confinement was varied, all other parameters being held constant. Continents were short (in a NS direction) and indenters wide (Fig. 3). The results show that lateral confinement is a critical factor in governing the relative amounts of thickening and lateral escape.

First, if the continent is confined between totally rigid and stationary lateral walls (Model 7), indentation produces crustal thickening in a plateau region in front of the indenter (Fig. 3, top row), without any lateral escape ($S = 0$, where S has been defined in the section on Analysis of Results). Arcuate thrust belts form in the uppermost brittle layer. The sense of overthrusting is sometimes away from the indenter (forethrusts), sometimes towards it (backthrusts). The first thrust forms close to the indenter; later ones serially away from it. Distant thrusts are bounded laterally by wrench zones containing wrench faults. Motion on individual thrusts tends to slow or cease, once crustal thickness has locally doubled. Presumably this is why new thrusts nucleate, making the plateau longer. Forethrusts and backthrust commonly form in conjugate pairs at different times. Where a forethrust faces a backthrust, a narrow topographic depression and a single fault trace are commonly the only surface expressions of a wide popdown wedge at depth. Between fault traces, broad topographic rises indicate popup wedges at depth. A detailed analysis of surface grids shows that slip vectors on arcuate faults are not simply directed NS, but rather have a radial disposition. Slip in these directions is observed to produce arc-parallel extension in the hanging walls of forethrusts and arc-parallel shortening in the hanging walls of backthrusts. Footwall deformation, if it occurs, is not observable, because of the lack of grids at depth. Across a popup wedge there is a gradient, from arc-parallel extension at the outer arc, to arc-parallel shortening at the inner arc. This implies a bending, with rotations of up to 20° about vertical axes, clockwise in the east, counterclockwise in the west. Bending strains do not result in visible minor faulting in this series of experiments.

In the second experiment (Model 3), the continent has a weak eastern margin (Fig. 3, middle row). Viscous confinement is provided by an uppermost layer of silicone 1 outside the continent. Indentation produces a plateau region of continental thickening and arcuate thrust belts, but this is less
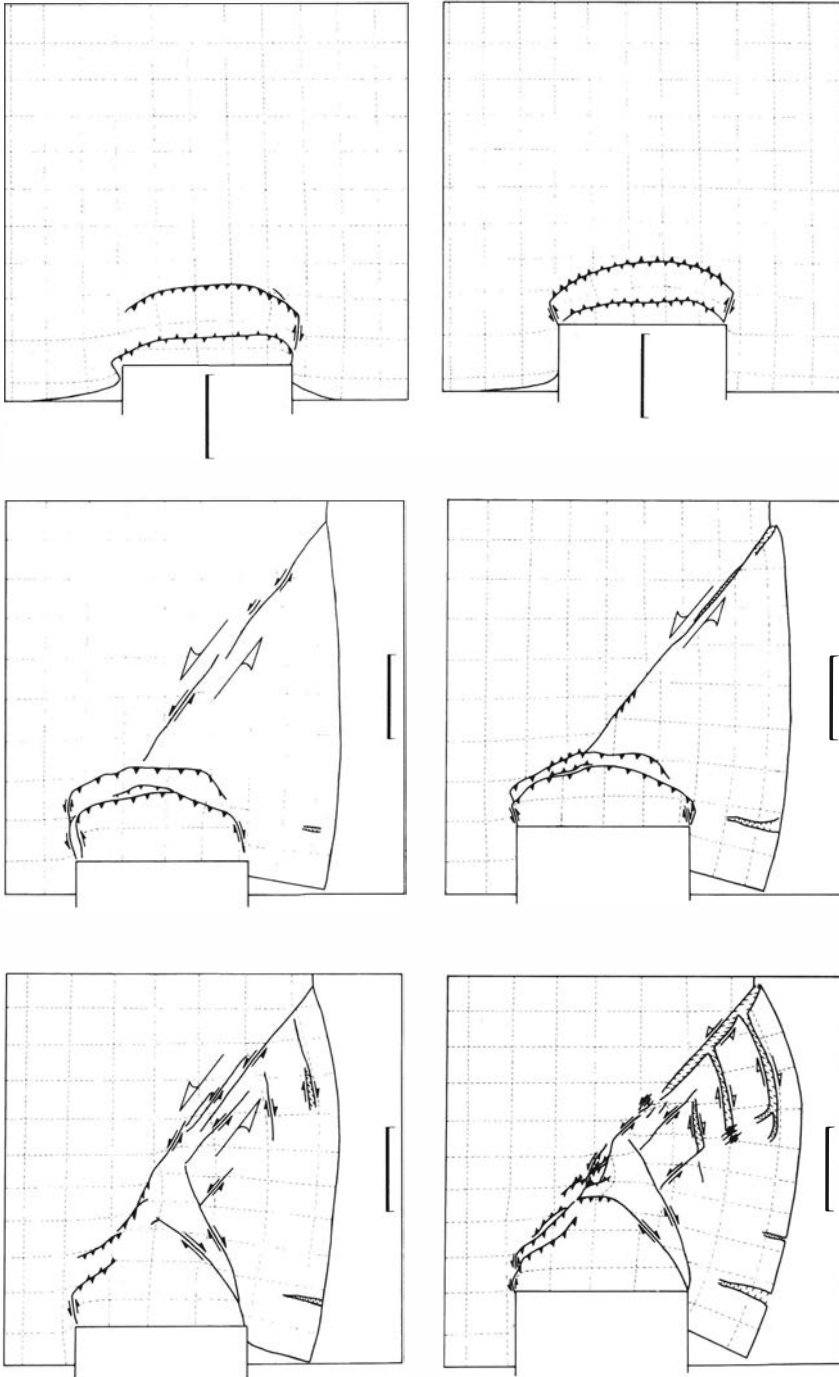
Fig. 3. Indentation patterns for 3 different degrees of lateral confinement at eastern (right-hand) margin. Top row (Model 7) is for rigid confinement, middle row (Model 3) for moderate confinement, bottom row (Model 2) for small confinement. Left-hand column shows 4 cm of indenter displacement; right-hand column, 8 cm. Continent is covered by originally orthogonal grid of passive lines spaced every 5 cm (dashed lines). Continental margins (continuous lines) are visible at right and at bottom. Grid is offset at fault traces (continuous lines), which are thrusts (triangles on hangingwall), strike-slip faults (sense indicated by opposing arrows), or normal faults (ticks on hangingwall). Scale bars are 10 cm long. For continental layering, see Table 1; for layering outside continents, see text.

symmetric than in the previous experiment. Thrusting is now less developed in the eastern part of the plateau (notice the lack of backthrusts). A significant part of the forward motion of the indenter is taken up by eastwards escape of a triangular block, the SE corner of the continent. The mechanism of escape is strike-slip faulting. A straight left-lateral wrench zone nucleates at the NW corner of the plateau and propagates rapidly northeastwards, until it intersects and offsets the continental margin. Simultaneously, right-lateral strike-slip motion occurs on the arcuate thrusts, especially the northernmost one. The apex of the triangle, between these conjugate wrench systems, is extended eastwards and there is significant bending within the triangle as a whole, with bulging of the continental margin. At late stages, the bending is sufficient to produce radial traingular rift valleys at the margin. As the indenter and the plateau region advance together, the eastern triangle as a whole undergoes some clockwise rotation. Plateau and triangle keep in contact along an arcuate thrust, slipping like a ball-and-socket joint; whereas relative rotation between the triangle and the stable remainder of the continent is taken up by convergence across the SW part of the main wrench zone and divergence across its NE part. Accretion of new thrust slices into the plateau progressively consumes the SW end of the main wrench zone. Between the two stages illustrated, the proportion of lateral escape increases (from $S = 1$ to $S = 2$).

Finally, in the third experiment (Model 2, Fig. 3, bottom row), the eastern continental margin is even less confined (there is no silicone layer upon the glucose syrup). Indentation is mostly taken up by lateral escape ($S = \S$). There is no plateau region in front of the indenter. A main left-lateral wrench zone initiates at the western corner of the indenter and propagates rapidly northeastwards, as before. It is met by conjugate right-lateral wrench faults, propagating northwestwards from the eastern corner of the indenter. The central triangle so defined moves rigidly northwards in front of the indenter; whereas the eastern triangle is expelled eastwards, as before. Notice, as before, the bending of the eastern triangle and some overall clockwise rotation. The main wrench zone is convergent in the SW, with en-échelon thrusts and segmented wrench faults; whereas it is strongly divergent in the NE, with pronounced rift valleys. Notice that the wrench zone widens progressively, consuming the eastern triangle by formation of synthetic and antithetic rift-wrenches. The antithetic ones are nearly parallel to the continental margin.

2. *Various sizes of indenter and continent*

In a second series of 3 experiments, only the sizes of the indenter or the continent were varied, all other parameters being held constant. A moderate degree of confinement was chosen, so as to favour both continental thickening and lateral escape. Both processes in fact occurred (Fig. 4), but their relative proportions and the detailed patterns of faults were different from one experiment to the next.

The first experiment (Model 3) has already been described, but a more advanced stage is here included, for better comparison with the other experiments (Fig. 4, top row).

In the second experiment (Model 4), the continent is as before, but the indenter is half as wide (Fig. 4, middle row). As a result, the plateau zone of thickening is narrower than before, but it is also longer towards the N, less symmetric and has more thrusts. The main left-lateral wrench zone is more complex. In the SW, it is strongly overtaken by the accreting plateau and becomes convergent. In the NE, two well-spaced synthetic wrench faults form; then the slice between them is cut by a series of closely-spaced antithetic wrench faults that rotate by a domino mechanism. The escaping eastern triangle bends and also rotates clockwise by as much as 20°, the previously described ball-and-socket mechanism being efficient against highly curved arcuate thrusts. The proportion of lateral escape is given by $S = 0.9$.

Finally, in the third experiment (Model 5), the continent is longer than before, but the indenter is equally narrow (Fig. 4, bottom row). Possibly because of the extra space available to the north, the main left-lateral wrench zone propagates northeastwards at a more acute angle, meeting the continental margin at a more northerly point. The escaping triangle is thus longer and becomes less strongly bent; but displacements on the main left-lateral wrench zone are greater than previously. Notice the zone of conjugate wrench faults immediately north of the plateau. There is only one complete arcuate thrust belt. The proportion of crustal thickening is moderate at an early stage ($S = 0.7$) and decreases at a late stage. This suggests that the greater amount of space available northwards within the continent has led to more lateral escape and less crustal thickening in the final stage.

In spite of the differences between these three experiments, there are broad similarities. There is always (i) a plateau region of thickened crust in front of the indenter, (ii) one major left-lateral wrench zone, that initiates at the western edge of the plateau and propagates out to the continental margin, and (iii) an eastern triangle that escapes
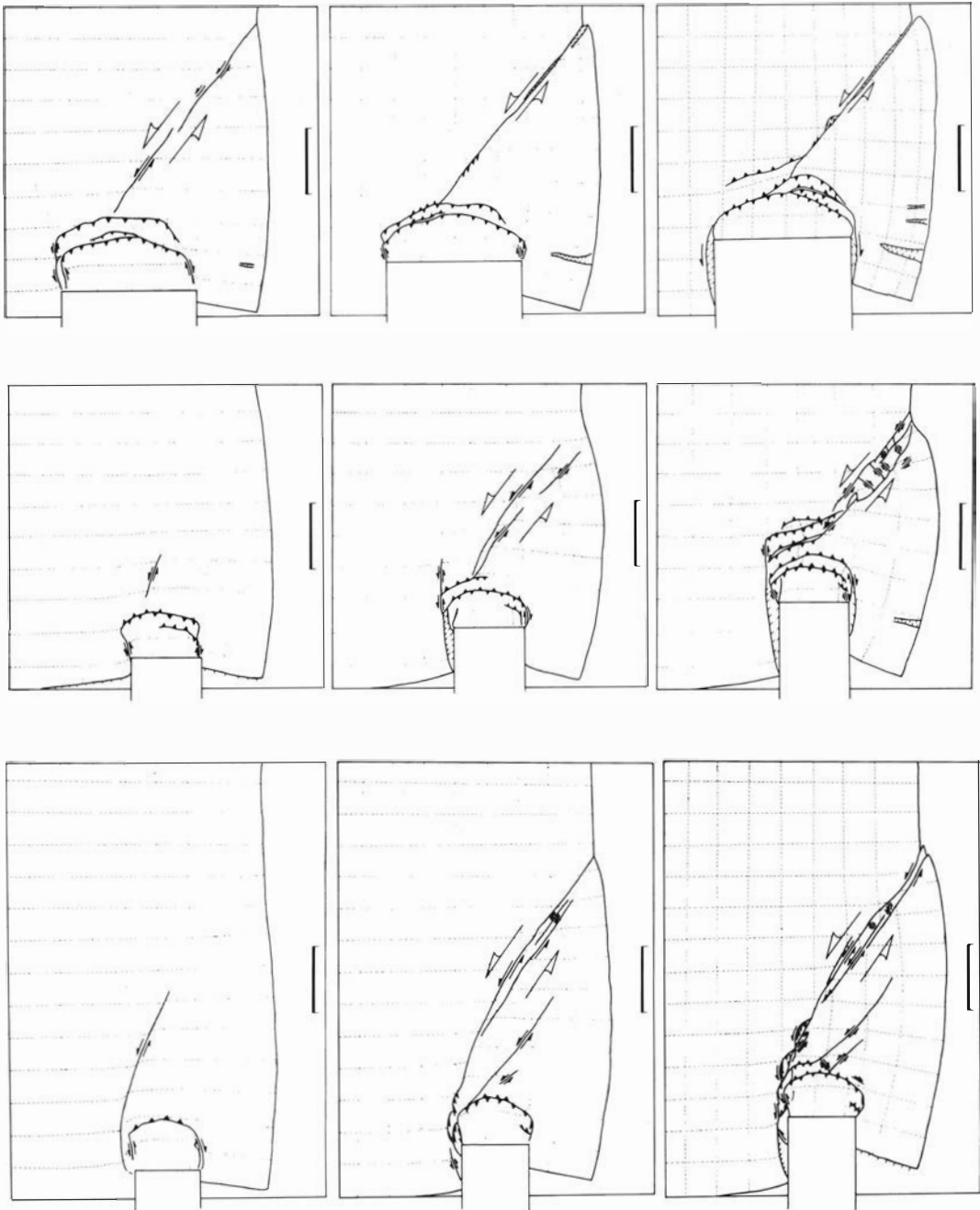
Fig. 4. Indentation patterns for 3 different shapes of indenter and continent. In Model 3 (top row), indenter is wide and continent is short; in Model 4 (middle row), indenter is narrow and continent is short; in Model 5 (bottom row), indenter is narrow and continent is long. Indenter displacements are 4 cm (left column), 8 cm (middle column) and 12 cm (right column). Same symbols as Fig. 2.
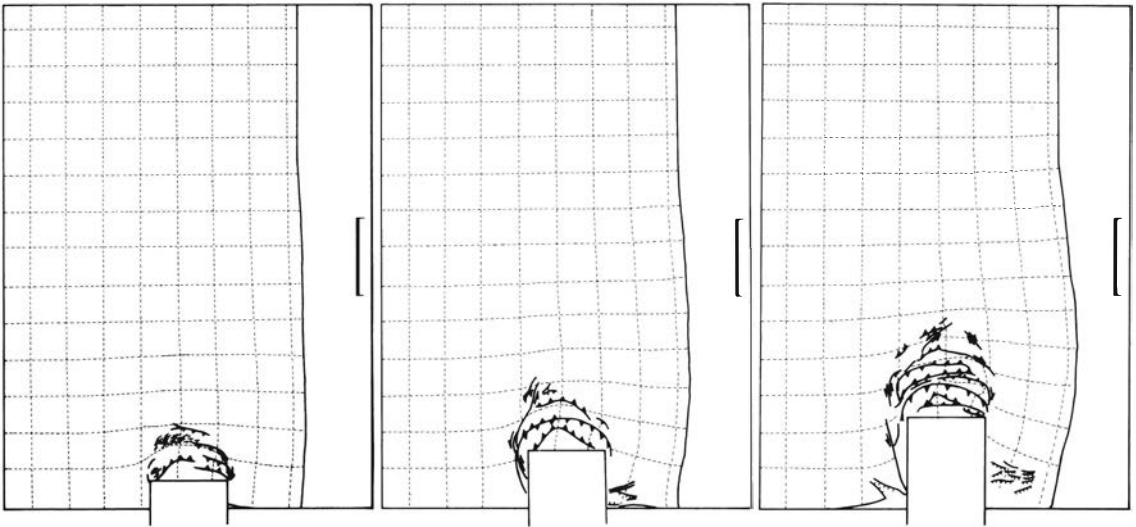
Fig. 5. Indentation pattern for long continent, narrow indenter and stiff mantle lithosphere under both continental and oceanic crust (Model 6). Same symbols as Fig. 2. See text for details.

eastwards, while bending somewhat and rotating on average clockwise.

3. Long continent, narrow indenter, various rheologies and lateral confinements

Only 2 experiments have so far been done in a series where a long continent with an eastern margin is deformed by a narrow indenter. The aim is to investigate the effects of various lithospheric rheologies and lateral confinements. One experiment has already been described (Model 5, Fig. 4).

The second experiment (Model 6, Fig. 5) differs from the first in that the entire model has an extra lithospheric layer (silicone 2, Table 1) representing a stiff upper mantle under both continental and oceanic crust. As a result, indentation produces crustal thickening, but almost no eastward escape, apart from some bending and bulging of the margin ($S = 0.4$). The faults in the plateau region are dominantly thrusts. Some conjugate wrench faults appear in front of the plateau, but displacements upon them are not large. On the basis of other experiments not described here (Davy, 1986), we attribute this pattern of deformation to the viscous lateral confinement provided by the layer of silicone 2, either directly at the continental margin, or indirectly via basal drag below the continental crust.

4. Long continent, very weak confinement

One experiment (Model 1) has been done to investi-

gate conditions of very weak confinement (Fig. 6). The continent is long and there are no silicone layers outside it. Underneath the continental crust there is no mantle lithosphere. Somewhat surprisingly perhaps, indentation produces almost no lateral escape. Plateau formation and crustal thickening are in this experiment preceded by rifting and right-lateral wrenching along a zone of weakness that forms at the eastern edge of the indenter and propagates northwards. Later this line becomes the eastern boundary of the accreting plateau region. Presumably the orientation and divergent nature of the zone of weakness are due to the very weak confinement at the continental margin and the tendency of the continent to spread eastwards under its own weight (see Vendeville et al., 1987 for a descritption of such spreading in physical models). Once formed, the zone of weakness functions mainly as a wrench, partitioning the deformation and presumably the stress field.

5. Deformable indenter, rigidly confined continent

A last set of 2 experiments was designed to see if rigidly confined large continents (same structure as that of Model 7, Fig. 3) can also be indented by smaller continents that have the same structure and rheology and so are themselves potentially deformable. Which will deform, the large or the small continent? In nature, small continents such as India appear to be laterally supported by strong oceanic
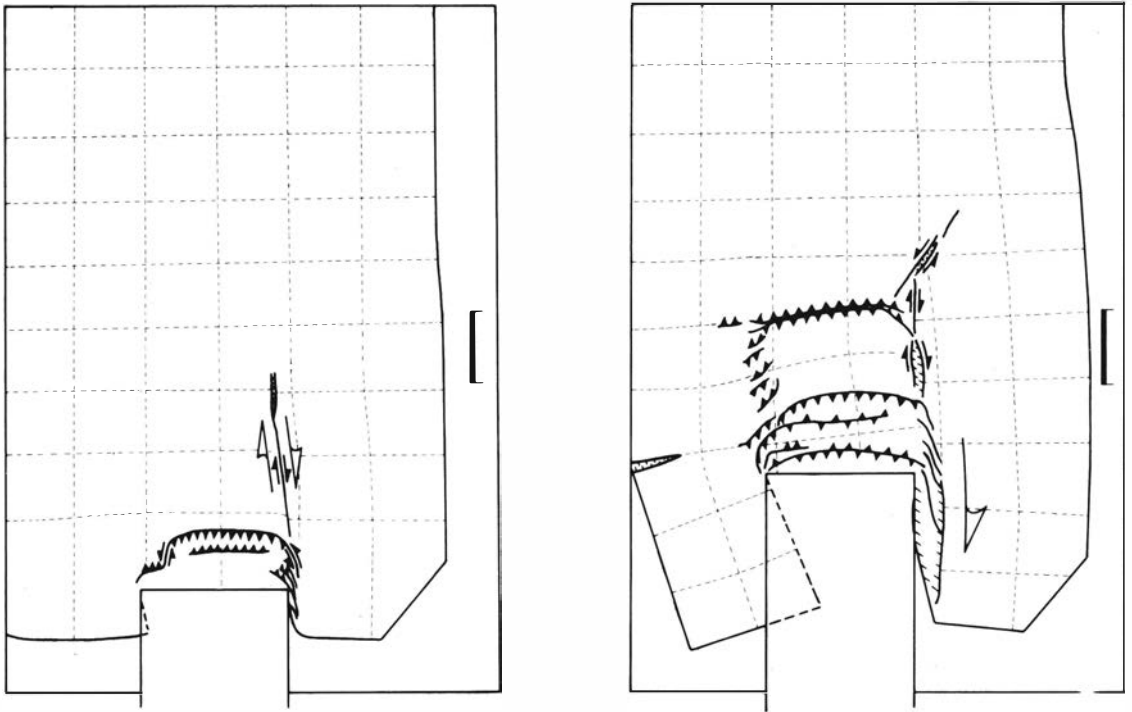
Fig. 6. Indentation patterns for long continent under very weak lateral confinement (Model 1). Same symbols as Fig. 2.

lithosphere. Hence we chose two kinds of rigid lateral boundaries for the small model continents.

In the first experiment, the small continent is supported to the south by a rigid rear wall and to east and west by tense flexible belts wound around stationary wheels (Model 8, Fig. 7, top row). The rigid rear wall is fixed to the belts and advances with them, carrying the small continent northwards. The belts provide lateral support, but only as far as the large continent. Initially there is no discontinuity between small and large continent: both form one continuous T-shaped plate. As the rearwall and belts advance northwards, a first arcuate backthrust forms, spanning the stem of the T. Material to the south of this is henceforth referred to as the small continent; material to the north, the large continent. At further stages in the experiment, the small continent is observed to indent the large continent, even though it advances beyond its supporting lateral belts. Indentation produces crustal thickening within the large continent alone. New arcuate back-thrusts form serially northwards, producing a plateau region. Notice that the thrusts are all convex northwards. The small continent does not deform. The lateral sutures between small and large continent are divergent wrench zones.

The second experiment differs from the first in that the small continent is laterally supported, not by belts, but by thin rigid plates that advance with it into the large continent (Model 9, Fig. 7, bottom row). As before, a first backthrust forms across the stem of the T; but this time, it is slightly convex to the south. Indentation causes crustal thickening, mainly in the large continent. The plateau is bounded in the north by a forethrust, convex to north; in the south by backthrusts, convex to south. In the final stages of the experiment, backthrusting propagates into the small continent.

In conclusion, a small continent can indent a large one, even through both have the same material properties, provided the small continent has lateral support. This lateral support appears to make the smaller continent stronger.

Discussion

In our experiments, the pattern of deformation depends upon the degree of lateral confinement, the sizes of continent and indenter, the rheological structure of the continent and also the rigidity of the indenter. The degree of lateral confinement appears
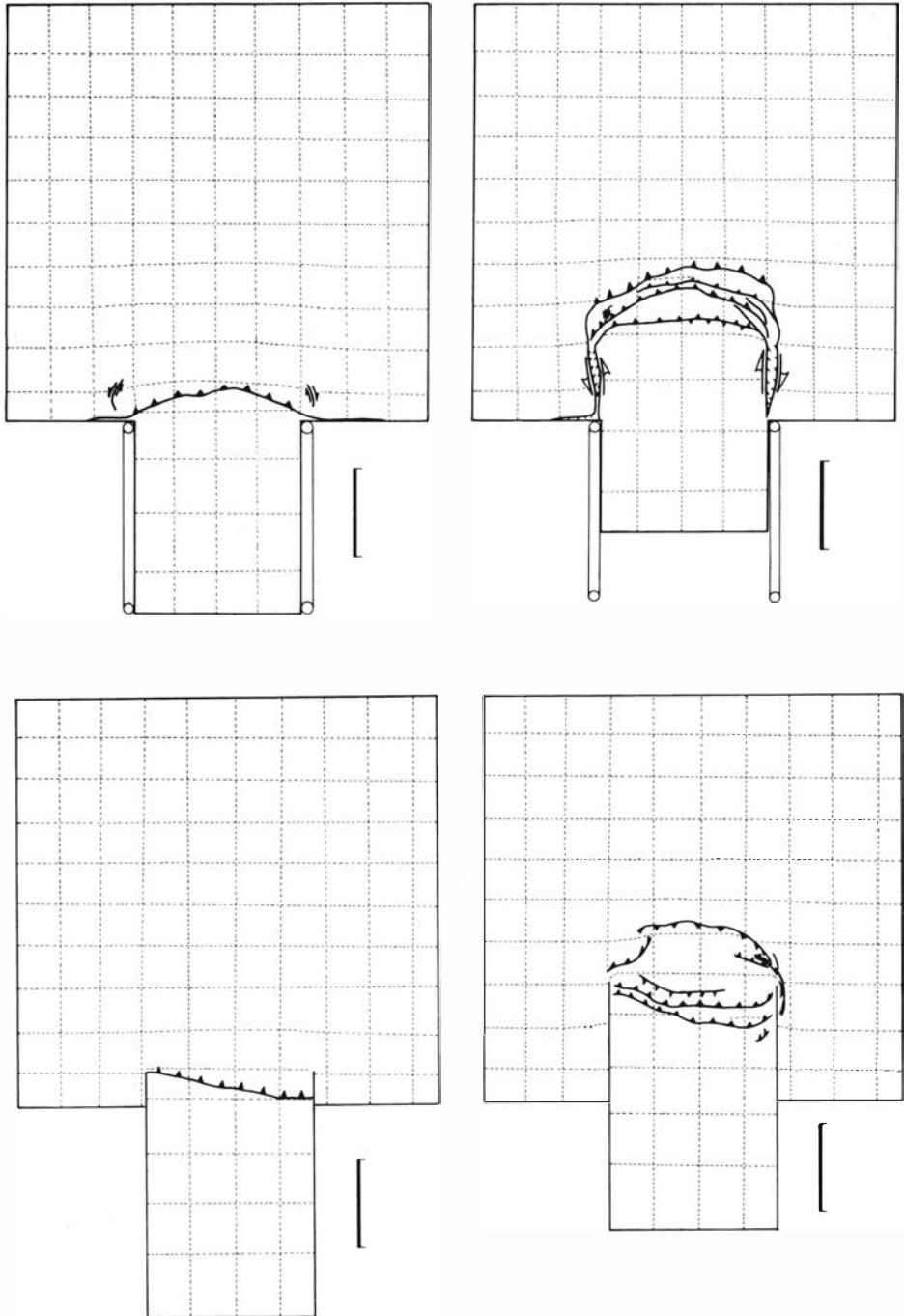
Fig. 7. Indentation patterns for rigidly confined continent and deformable indenters. In Model 8 (top row), indenter advances with confining belts that do not enter large continent; in Model 9 (bottom row), indenter advances into continent together with rigid confining plates. Same symbols as Fig. 2.
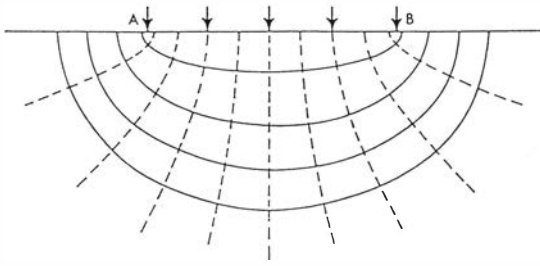
Fig. 8. Stress trajectories for uniform loading over a strip AB on the surface of a semi-infinite elastic region (after Jaeger & Cook 1971, page 288). Trajectories are confocal ellipses and hyperbolae.

to be especially important in governing the relative amounts of crustal thickening and lateral escape.

In confined continents penetrated by relatively small indenters, crustal thickening predominates. If one ignores the highly localized deformation due to faulting, the regional pattern of crustal thickening in our models is similar to that obtained numerically by England & McKenzie (1982), Houseman & England (1986) and Cohen & Morgan (1987), assuming viscous behaviour with no strain-softening. It is also similar to the numerical results of Vilotte et al. (1982) for the ideal situation of plane stress. On the other hand, all these results are very different from the models of Tapponnier & Molnar (1976), Tapponnier et al. (1982) or those of Vilotte et al. (1982) that assume plane strain.

There is a very simple analytical solution that we believe can adequately explain the initiation of arcuate thrust belts in front of a narrow indenter. This is the solution for the stress distribution in an elastic half-space, subjected to a line-load over a strip of finite length (Fig. 8). The solution is valid for both plane stress or plane strain, depending on how the elastic constants and boundary displacements are defined. The stress trajectories in front of the indenter are confocal ellipses and hyperbolae; whereas equal values of principal stresses lie along circles. For plane stress, the solution predicts that failure will occur along arcuate thrust-surfaces with elliptic traces. Our experimental observations seem to fit this prediction fairly well, especially in the early stages of deformation. The elastic solution also predicts that slip vectors at failure will be normal to thrust traces and hence have a roughly radial distribution. Once again, this prediction seems to be verified in our experiments. Both the experiments and the elastic solution show that a concentrated boundary load, such as produced by a narrow indenter, leads to a roughly radial stress field with a high degree of arc-parallel confinement near the indenter. We refer to this feature as local self-confinement.

Our experiments seem to show that local self-confinement breaks down, either as the indenter becomes too wide relative to the continent, or as the lateral confinement upon the continent is relaxed. These two effects could be incorporated into more complex elastic models, but we have not explored these possibilities as yet. Instead we fall back on an even simpler model, in which we assume that the state of stress away from the indenter is effectively homogeneous, with an east-west principal stress σ_1, equal to the lateral confinement, and a north-south principal stress, $\sigma_c' = \sigma_c \cdot L_p/L_2$, where σ_c is the indenting stress and L_p/L_2 is a geometrical factor expressing the relative widths of piston and continent (Fig. 1). On this basis, we have calculated the ratio $R = \sigma_c'/\sigma_1$ for the various experiments (column 7, Table 2). The stress σ_1 has been calculated using the rheological properties of the material outside the eastern continental margin; whereas σ_c has been calculated assuming a constant deformation rate for the continent. High values of R indicate weak confinement or wide indenters; low values indicate strong confinement or narrow indenters. We see that lateral escape in the models increases for high values of R. Hence R seems to be a simple yet effective measure for predicting the relative amounts of lateral escape and crustal thickening.

At high values of R, deformation in our experiments approximates a plane strain, except in the immediate vicinity of the indenter. Lateral escape thus predominates over crustal thickening. Nevertheless we have not observed successive lateral extrusion of blocks as described by Tapponnier et al (1982) for models deformed in strict plane strain. In our models, there is only one major left-lateral wrench zone, emanating from the western tip of the indenter. This result is important for discussing the relevance of the various models to the tectonics of Asia (see Part 2 of this series of papers).

REFERENCES

Argand, E. 1924. La tectonique de l'Asie. *Congres Geologique International, Comptes Rendus de la XIII Session, en Belgique,* 1922, Premier fascicule, 1–596.
Brace, W.F. and Kohlstedt 1980. Limits on lithospheric stress imposed by laboratory experiments. *J. Geophys. Res, 85,* 6248–6252.

Carter, N.L. 1976. Steady state flow of rocks. *Rev. Geophys. Space Physics, 14* (3), 301−360.

Carter, N.L. & Tsenn, N.C. 1987. Flow properties of continental lithosphere. *Tectonophysics, 136* (1/2), 27−64.

Cohen, J.C. & Morgan, R.C. 1987. Intraplate deformation due to continental collisions: a numerical study of deformation in a thin viscous sheet. *Tectonophysics, 132,* (1/3), 247−260.

Davy, P. 1986. Modelisation thermo-mecanique de la collision continentale. *Mém. Doc. Centre Arm. Et. Struct. Socles, Rennes, 8,* 233 p.

England, P.C. 1982. Some numerical investigations of large scale continental deformation. In: *Mountain Building Processes* (ed. by K. Hsü), Academic Press, Orlando, Fla., 129−139.

England, P. & Houseman, G. 1986. Finite strain calculations of continental deformation. 2. Comparison with the India-Asia collision zone. *J. Geophys. Res., 91,* B3, 3664−3676.

England, P.C. & McKenzie, D.P. 1982. A thin viscous sheet model for continental deformation. *Geophys. J.R. Astron. Soc., 70,* 295−321.

England, P.C. & McKenzie, D.P. 1983. A thin viscous sheet model for continental deformation (correction to: A thin viscous sheet model for continental deformation, Geophys. J.R. Astron. Soc. 70, 295−321, 1982). *Geophys. J.R. Astron. Soc., 73,* 523−592.

Goetze, C. & Evans, B. 1979. Stress and temperature in the bending lithosphere as constrained by experimental rock mechanics. *Geophys. J.R. Astron. Soc., 59,* 463−478.

Heard, H.C. 1976. Comparison of the flow properties of rocks at crustal conditions. *Phil. Trans. R. Soc. Lond.,* A 283, 173−186.

Horsfield, W.T. 1977. An experimental approach to basement-controlled faulting. In: Fault Tectonics in N.W. Europe (ed. by R.T.C. Frost and A.J. Dikkers), *Geologie en Mijnbouw, 56* (4), 363−370.

Houseman, G. & England, P. 1986. Finite strain calculations of continental deformation. I. Method and general results for convergent zones. *J. Geophys. Res., 91,* B3, 3651−3663.

Hubbert, M.K. 1937. Theory of scale models as applied to the study of geologic structures. *Geol. Soc. Am. Bull., 48,* 1459−1520.

Jaeger, J.C. & Cook, N.G.W. 1971. *Fundamentals of rock mechanics.* Chapman & Hall, London, 515 p.

Kirby, S.H. 1983. Rheology of the lithosphere. *Rev. Geophys. Space Phys., 21* (6), 1458−1487.

Kirby, S.H. 1985. Rock mechanic observations pertinent to the rheology of the continental lithosphere and the localization of strain along shear zones. *Tectonophysics, 119,* 1−27.

Mandl, G., De Jong, L.N.J. & Maltha, A. 1977. Shear zones in granular material. *Rock Mechanics, 9,* 95−144.

Molnar, P. & Tapponnier, P. 1975. Cenozoic tectonics of Asia: effects of a continental collision. *Science, 189,* 419−426.

Molnar, P. & Tapponnier, P. 1981. A possible dependence of tectonic strength on the age of the crust in Asia. *Earth Planet. Sci. Lett., 52,* 107−114.

Peltzer, G. 1987. Contribution à l'étude de la collision Inde-Asie 1) approche expérimentale, équilibre entre épaississement crustal et extrusion latérale 2) estimation des déplacements quaternaires sur le bord nord du Tibet., Thèse d'Etat, Université de Paris VII, 400 p.

Peltzer, G. 1988. Experimental approach in a centrifuge of large scale continental tectonics in Asia. *This volume.*

Peltzer, G. and Tapponnier, P. 1988. Formation and evolution of strike-slip faults, rifts and basins during the India-Asia collision: an experimental approach. *J. Geophys. Res.,* in press.

Ramberg, H. 1967. *Gravity, deformation and the Earth's Crust.* Acad. Press, London, 214 p.

Ranalli, G. & Murphy, D.C. 1987. Rheological stratification of the lithosphere. *Tectonophysics, 132* (4), 281−296.

Tapponnier, P., Molnar P. 1976. Slip-line field theory and large-scale continental tectonics. *Nature, 264,* 319−324.

Tapponnier, P., Peltzer, G., Le Dain, A.Y., Armijo, R. & Cobbold, P.R. 1982. Propagating extrusion tectonics in Asia: new insights from simple experiments with plasticine. *Geology, 10,* 611−616.

Tapponnier, P., Peltzer, G. & Armijo, R. 1986. On the mechanics of the collision between India and Asia. In: Collision Tectonics (eds. M.P. Coward & A.C. Ries), *Geological Society of London, Spec. Publ., 19,* 115−157.

Tsenn, M.C. & Carter, N.L. 1987. Upper limits of power law creep of rocks. *Tectonophysics,* 136 (1/2), 1−26.

Vendeville, B., Cobbold, P.R., Davy, P., Brun, J.P. & Choukroune, P. 1987. Physical models of extensional tectonics at various scales; In: Continental Extension Tectonics (ed. by M.P. Coward, J.F. Dewey & P.L. Hancock), *Geol. Soc. of London, Spec. Publ., 28,* 95−107.

Vilotte, J.P., Daignieres, M. & Madariaga, R. 1982. Numerical modelling of intraplate deformation: simple mechanical models of continental collision. *J. Geophys. Res., 87,* B13, 10709−10728.